Computer Simulation of Primary Photosynthetic Reactions — Compared with Experimental Results on O_2-Exchange and Chlorophyll Fluorescence of Green Plants

Christian Holzapfel

Institut für Chemie II, Kernforschungsanlage Jülich

and

Robert Bauer §

Institut für Physikalische Chemie der Technischen Hochschule Aachen

(Z. Naturforsch. **30 c**, 489–498 [1975]; received March 3/April 18, 1975)

Primary Photosynthetic Electron Transport, Computer Simulation, Fluorescence Induction, Oxygen Exchange Transient

A computer model describing the "Z-scheme" of photosynthetic electron transport in terms of reduction and oxydation of coupled redox pools was built up. Starting from a certain initial state corresponding to the dark adapted state of the photosynthetic system the reduction and reoxidation levels of the pools were calculated during adaptation of the system to a steady state in the light. The changes of calculated redox levels were compared with experimental results of fluorescence and oxygen evolution induction curves. It is shown that the transients in prompt fluorescence and oxygen evolution can be described by reduction and reoxidation of the primary electron acceptor pool and the electron donor pool of photosystem II due to reduction and oxidation of the other pools during adaptation to light. The first depression D in the fluorescence induction curve is explained by the existence of a redox pool X between the primary electron acceptor pool Q of photosystem II and plastoquinone. It is shown that DCMU blocks the electron flow between Q and X. Furthermore, it is shown that the inhibitor DBMIB probably not only blocks the electron flow but also causes a successive disconnection of the plastoquinone pool from the electron transport chain.

Introduction

Many data have been collected in the last years concerning the electron transport in the primary photosynthetic processes. This resulted in several conceptions about the pathway of electron flow. Therefore, it seems useful to build up a model of electron flow, in which the concepts can be checked quantitatively. Such a model connects certain input data, *e. g.* light intensity, oxygen, and carbon dioxide concentration, and yields output data which can be compared with experimental data. The comparison gives us information about whether the model has to be revised or in which points it has to be changed.

If the computer model is in accordance with all significant experimental data, it may be allowed to draw quantitative kinetical conclusions on reactions which have not yet been experimentally approached ore are still in discussion.

In the primary photosynthetic reactions of green plants electrons delivered from the water splitting reaction are transferred with the aid of two primary photochemical reactions (light reaction I resp. II) – connected in series with several electron transfer components – to the terminal electron acceptor $NADP^+$. The electron transfer to $NADP^+$ causes an electrochemical potential difference across the thylakoid membrane which provides energy for the phosphorylation reaction, *i. e.* the synthesis of ATP from ADP and P_i [1]. Reduced NADP, together with ATP serves to drive the Calvin-Benson cycle which is responsible for the reduction of CO_2 into sugar.

In the functional membrane of photosynthesis the electron transport chain from water to $NADP^+$ has vectorial properties [2]. The electron transport can be represented schematically in an energy diagram by a chain of coupled redox systems, first proposed by Hill and Bendall in 1960. In this so called "Z-scheme" the electron transferring intermediates are arranged according to their individual redox potentials. It is known that these redox inter-

Requests for reprints should be send to Dr. Chr. Holzapfel, ICH II, KFA-Jülich,, *D-5170 Jülich*.

§ Present address: Ruhr-Universität Bochum, Lehrstuhl für Biochemie der Pflanzen, D-4630 Bochum.

mediates are present in different quantities and have different kinetic properties.

The induction phenomena of oxygen evolution [3, 4] and fluorescence of green plants subjected to a sudden change in light intensity, *e. g.* from dark to light, is one key to the understanding of the primary photosynthetic process [5]. Fluorescence and oxygen evolution show typical and well reproducable transients which can last from milliseconds to several minutes. The induction phenomena vary quantitatively with species and with pretreatments. However, qualitatively they show the same features typical for all green plants.

Several attempts were made to describe the induction phenomena in terms of the model mentioned above. Analytic descriptions were presented by Malkin and Kok [6, 7] and by Munday and Govindjee [8] in which the model was simplified in order to obtain an analytical solution of the equations. However, to get numerical solutions of a system of equations which can not be solved analytically, we have to use a computer.

Simple systems of equations can be handled by an analog computer [9]. To expand the power of computer simulations to more complicated systems it is necessary to use a digital computer. In this paper we present a modelling of the Z-scheme on the IBM/370-168 at the KFA-Jülich.

Description of the Model

The Z-scheme of the primary processes of photosynthesis can be described in terms of coupled redox pools of the intermediates. Electrons are pumped by the two photosystems PS II and PS I (Fig. 1) from the first water splitting electron donor Z of PS II to the terminal electron acceptor of PS I, $NADP^+$, from where the dark reactions start.

The state of one of the pools in the redox chain, denoted B, is characterized by its amount of reduced molecules $[B^-]$ and by its total size $[B_0]$. The remaining amount of nonreduced molecules is

$$[B] = [B_0] - [B^-]. \tag{1}$$

The pool B is reduced by the preceeding pool A which is oxidized by the transfer of electrons from A to B. B is reoxidized by reducing the next pool C in the chain

$$A^- + B + C \rightarrow A + B^- + C \rightarrow A + B + C^-. \tag{2}$$

The kinetics of reduction and reoxidation of B is described by a second order rate equation

$$\frac{d}{dt}[B^-] = \alpha[A^-][B] - \beta[B^-][C]. \tag{3}$$

The pumping effect of the photosystems PS II and PS I is described by setting α proportional to the amount of excited centers [PS II*] or [PS I*].

The two photosystems are also described as pools of centers, which can be excited by light,

$$\text{PS II} \rightarrow \text{PS II}^* \quad \text{and} \quad \text{PS I} \rightarrow \text{PS I}^* \tag{4}$$

according to

$$\frac{d}{dt}[\text{PS II}^*] = k_2 \cdot I \cdot [\text{PS II}] - k_3 \cdot [\text{PS II}^*], \tag{5}$$

where I is the intensity of light.

The steady state value of excitation is

$$[\text{PS II}^*]_s = [\text{PS II}_0] \cdot \left(1 + \frac{k_3}{k_2 I}\right)^{-1}. \tag{6}$$

The excitation of PS I is described in the same way.

For the purpose of simplicity we describe the water splitting pool Z by its oxidation instead of reduction,

$$Z \rightarrow Z^+. \tag{7}$$

The simplest way to describe the output of oxygen is to set the oxygen evolution proportional to the amount of oxidized Z. Z is oxidized by PS II which pumps electron from Z to Q according to its amount of excited molecules [PS II*], and Z is reduced again by the water splitting process:

$$\frac{d}{dt}[Z^+] = k_1 \cdot [\text{PS II}^*] \cdot [Z] \cdot [Q] - k_0 \cdot [Z^+]. \tag{8}$$

The rate of oxygen evolved is

$$O_2 - \text{evol.} = \tfrac{1}{4} k_0 \cdot [Z^+], \tag{9}$$

since four electrons must be transfered by Z for each O_2 molecule released from water [12–14].

The quencher Q is reduced by the same pumping effect and oxidized by the next pool X

$$\frac{d}{dt}[Q^-] = k_1 \cdot [\text{PS II}^*] \cdot [Z] \cdot [Q] - k_4 \cdot [Q^-] \cdot [X]. \tag{10}$$

The next pool X is reduced by Q^- and reoxidized by the plastoquinone pool P Q,

$$\frac{d}{dt}[X^-] = k_4 \cdot [Q^-] \cdot [X] - k_5 \cdot [X^-] \cdot [\text{P Q}]. \tag{11}$$

This way we can describe the reduction and oxidation of all the pools according to the model in Fig. 1 by a system of differential equations.

Four postulated protolytic reactions (two proton-uptake reactions at the outer side, *i. e.* the reduction of P Q and $NADP^+$, and two proton releasing reactions in the inner phase of the membrane, *i. e.* the water splitting reaction and the P Q-oxidation) lead to a pH-difference, ΔpH, across the thylakoid membrane, which leads to an increase of ATP [2]. $NADPH_2$ is oxidized by dark processes which is described by an electron flow f and by the output of (CH_2O).

The output of fluorescence light is described by the proportionality between intensity of emitted light and amount of reduced quencher Q,

$$\text{Fluorescence} \sim [Q^-]. \qquad (12)$$

The pool sizes and rate constants are chosen according to measured values from literature as far as known. *I. e.* all the pools but P Q have the same size, only P Q is 6 times bigger.

Furthermore, the reduction time of P Q is

$$\tau_{red} = \{k_5 \cdot [P\,Q_0]\}^{-1} = 0.6 \times 10^{-3}\ \text{sec},$$

and the reoxidation time of P Q is

$$\tau_{ox} = \{k_6 \cdot [\text{Cyt}\,f_0]\}^{-1} = 20 \times 10^{-3}\ \text{sec}\ [1, 15].$$

The adjustment of unknown parameters to correct relationship between input and output is one source of further information about the system described by the model.

Results of Calculation and Comparison with Experimental Data

Integrating the system of differential equations numerically with a simple Newton method we can follow the reduction and reoxidation of the pools beginning from a certain state corresponding to the dark adapted state of the photosynthetic system through the phases of adjustment untill a steady state has been established for all the pools. This gives us a description of induction phenomena in the change of the redox state of the pools. We can compare changes in the oxidation of the pool Z, *i. e.* the water splitting complex, with the experimental induction phenomenon of oxygen evolution. The change in the redox state of pool Q can be compared with the induction phenomenon of fluorescence, *i. e.* the Kautsky effect [16].

In Fig. 2 a the change of $[Q^-]$ shows the characteristics of the fluorescence induction curve as measured in *e. g.* the green algae *Chlorella* or *Scenedesmus* [17, 18] (Fig. 2 b). Fig. 2 a also shows the parallel change of $[Z^+]$, which shows the characteristics of the oxygen induction with the first gush at about the same time as the first depression D occurs in the fluorescence induction and with the minimum occuring at the same time as the maximum P occurs in the fluorescence induction [19, 20].

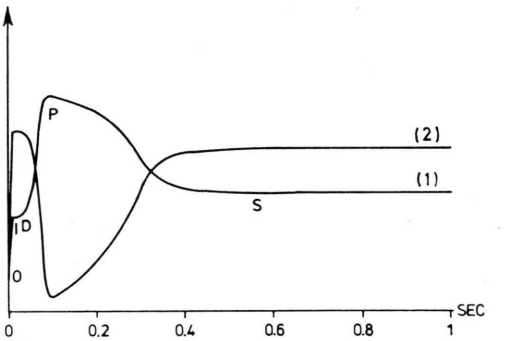

Fig. 2 a. Fluorescence (1) and oxygen evolution (2) induction curve calculated for a dark adapted photosynthetic system according to Fig. 1 without any block. Units of fluorescence and oxygen evolution are arbitrary.

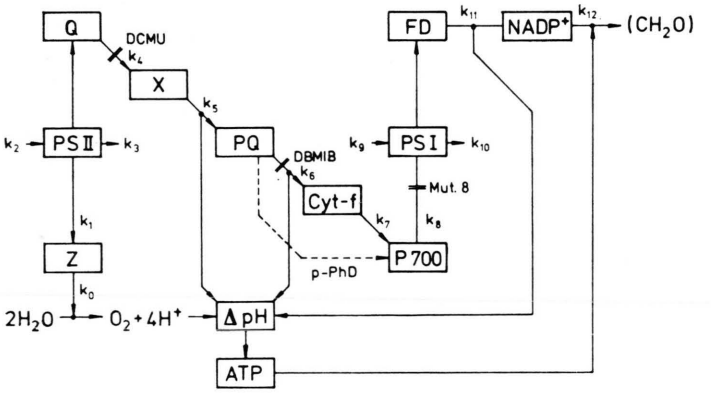

Fig. 1. Z-scheme of the photosynthetic electron transport chain from water to $NADP^+$. PS II and PS I, photosystem II and I; Z, water splitting system of PS II (primary donor); Q, quencher of fluorescence (primary acceptor of PS II), probably a special quinone [1]; X, probably Cyt b-559 [10, 11]; PQ, plastoquinone; Cyt-f, cytochrome f; P 700, reaction-center chlorophyll a_{700} of PS I; FD, Ferredoxin; DCMU, 3-(3,4-dichlorophenyl)-1,1-dimethylurea; DBMIB, 2,5-dibromo-3-methyl-6-isopropyl-*p*-benzoquinone; *p*-PhD, 1,4-phenylenediamine-dihydrochlorid.

In the model the first increase OID in the fluorescence reflects the initial filling of the empty pools Z and Q due to the pumping effect of PS II according to Eqns (8) and (10). Because of the empty pool X the flow of electrons out of Q increases in the same way as Q is filled up with electrons. The flux into Q from Z decreases because both Q and Z are exhausted, *i. e.* Q is progressively reduced and Z is progressively oxidized. At I and D the two fluxes, input to Q and output from Q are balanced.

The next increase from D to P in $[Q^-]$ is caused by the filling of the following pools X and P Q, which leads to a decrease of the efflux of electrons from Q, that means Q is further reduced up to the maximum P. Also, at the same time the input of electrons to Q and the oxidation of Z is decreased, *i. e.* the reduction of Z is increased due to the second term in Eqn (8), the water splitting process. This leads to the minimum in $[Z^+]$.

The further decrease of $[Q^-]$ from the maximum P to the steady state value S is caused by the increasing oxidation of the pools through PS I due to the increase of ΔpH and ATP, which leads to reoxidation of $NADPH_2$. In consequence this leads to reoxidation of FD and thus to an increase of the electron flux through PS I. As Q is reoxidized by this process the pool Z is also oxidized due to the increase of the electron flux from Z to Q by the first term in Eqns (8) and (10). The change of $[Q^-]$ and $[Z^+]$ thus reflect the filling and emptying of all the pools during adaptation to the steady state. The first part of the induction up to the maximum P is influenced by the pools close to PS II, *i. e.* Z, Q, X, and P Q. An important fact for the understanding of the first depression D in the fluorescence induction curve (and the contemporarily occuring first gush in the oxygen evolution) is the existence of the pool X.

The second part, the slower decrease from P to S, is caused by the slower dark reactions (consumption of $NADPH_2$ in the CO_2-assimilation reaction due to the increase of ATP).

With DCMU the electron flow is blocked between Q and X, which corresponds to $k_4 = 0$ in the model (Fig. 1). Fig. 3 a shows that in this case Q is reduced almost completely before the depression D occurs. This is also measured for the fluorescence induction curve in DCMU treated green algae [17] (Fig. 5 b). The first millisecond region of the increase of $[Q^-]$ shows that a block between X and

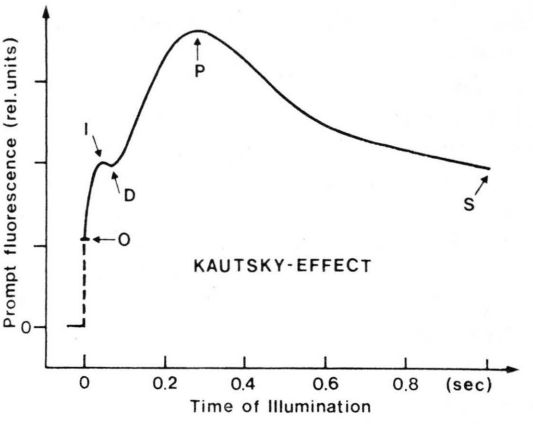

Fig. 2 b. Typical chlorophyll fluorescence induction curve of *Scenedesmus obliquus* at the onset of illumination. Temperature: 28 °C, light intensity 8 mW/cm². O, initial fluorescence; I, initial peak; D, dip; P, peak; S, almost steady fluorescence level [18].

P Q, *i. e.* $k_5 = 0$ does not influence the very first increase of $[Q^-]$ as compared to the unblocked case. The blocking between Q and X, *i. e.* $k_4 = 0$, shows a quicker increase of $[Q^-]$ as compared to the unblocked case in the millisecond region (Fig. 3 b). This quicker increase in the millisecond region fluorescence has also been measured in DCMU blocked *Scenedesmus* [17]. Thus it seems obvious that DCMU blocks the electron flow between Q and X rather than between X and P Q.

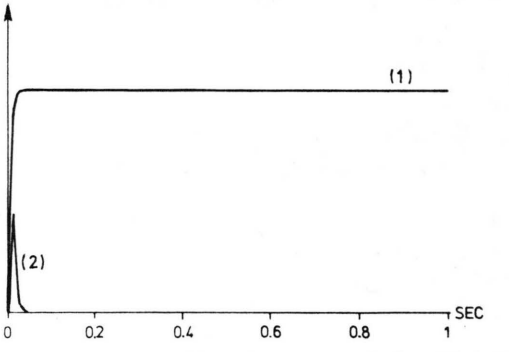

Fig. 3 a. Fluorescence (1) and oxygen evolution (2) induction curve calculated for a dark adapted photosynthetic system blocked between Q and X ($k_4 = 0$ in Fig. 1) according to DCMU block *in vivo*.

The pool Z shows a small increase of $[Z^+]$ and a quick return to zero due to the total reduction of Q.

Similar results are found in DCMU treated green algae which show an oxygen evolution at the beginning of a flash light regime [21].

With DBMIB the electron flow is blocked between P Q and Cyt f [23], which corresponds to $k_6 = 0$. If the flux is blocked here, the model shows that Q would be reduced completely before the maximum P occurs but still showing the depression D.

This is not in agreement with experimental results. In DBMIB treated algae (Fig. 4 d) and also in the PS I blocked mutant No. 8 of *Scenedesmus obliquus* [22] the fluorescence increases to its maximal value without showing the depression D [17, 18]. In order to get conformity with experimental findings we have to assume that DBMIB at high concentrations not only blocks the electron flux but also causes a successive disconnection of the reactive P Q to a high degree. This in expressed in the model as a successive reduction which is equivalent to a diminution of the P Q pool.

Also in mutant No. 8 in which the block in the electron transport probably corresponds to $k_8 = 0$ (Fig. 1) we have to assume that P Q is reduced or diminished to a high degree. The lack of P 700 in mutant No. 8 [22] is described by $[P\,700_0] = 0$, which has the same effect as $k_8 = 0$ or $k_7 = 0$ in the model. Fig. 4 a shows the change of $[Q^-]$ with $k_6 = 0$ for several values of the initial value of $[P\,Q^-]$. Fig. 4 b shows the change of $[Q^-]$ and $[Z^+]$ for $k_6 = 0$ and with $[P\,Q^-]_{init} = [P\,Q_0]$, *i. e.* 100% reduction. The pool Z shows a bigger gush of oxydation as compared to the case $k_4 = 0$ (Fig. 3 a) due to the total reduction of Q and X.

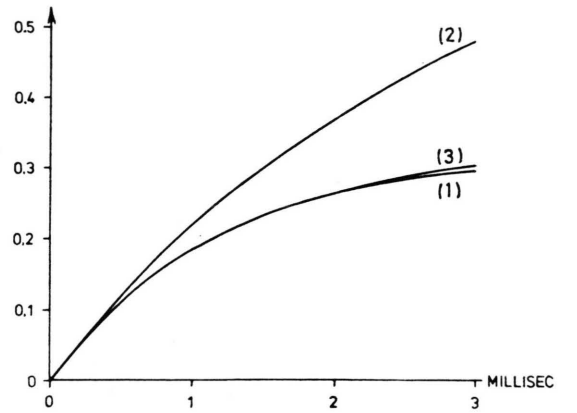

Fig. 3 b. Reduction of the quencher Q in the first few milliseconds calculated for a dark adapted photosynthetic system without any block (1), with $k_4=0$ (2), and with $k_5=0$ (3) in Fig. 1.

With *p*-phenylenediamine (*p*-PhD) the influence of DBMIB on fluorescence induction is abolished [18]. The explanation may be that *p*-PhD acts as a redox

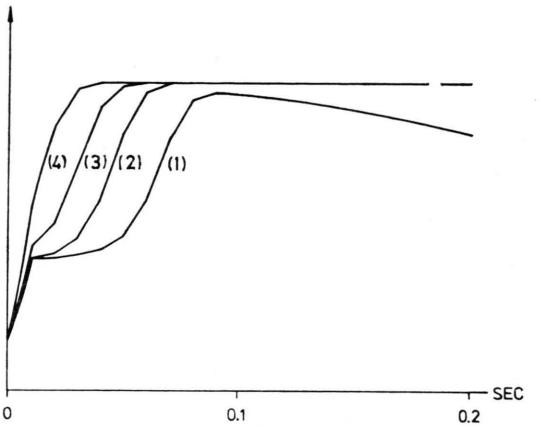

Fig. 4 a. First portion of the fluorescence induction curve calculated for a dark adapted photosynthetic system without any block (1) and with a block between PQ and Cyt f ($k_6=0$ in Fig. 1) and different initial reduction values of PQ: 50% reduced (2), 75% reduced (3), and 100% reduced (4).

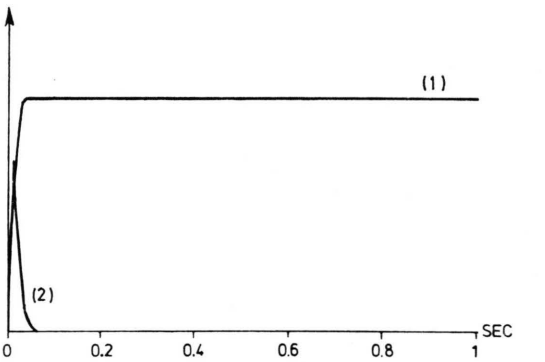

Fig. 4 b. Fluorescence (1) and oxygen evolution (2) induction curve calculated for a dark adapted photosynthetic system with $k_6=0$ (Fig. 1) according to DBMIB block *in vivo* with 100% initial reduction of PQ.

system which is able to mediate an artificial electron transport bypass of the DBMIB-inhibition site by transporting electrons from P Q to P 700, probably *via* plastocyanin [23]. Because of the conflicting data about the physiological role and the location in the electron transport chain relative to Cyt f and P 700, plastocyanin is not considered in the model.

Fig. 4 c shows the restored induction curves still with the block between P Q and Cyt f ($k_6 = 0$) but with a transfer of electrons from P Q to P 700 by an equation analog to (3) corresponding to the *p*-PhD shuttle.

Figs 4 d and 4 e show the experimental data of DBMIB treated *Scenedesmus obliquus* and the restoration of the fluorescence induction curve by *p*-PhD [18]. Fig. 4 f shows the induction curve of

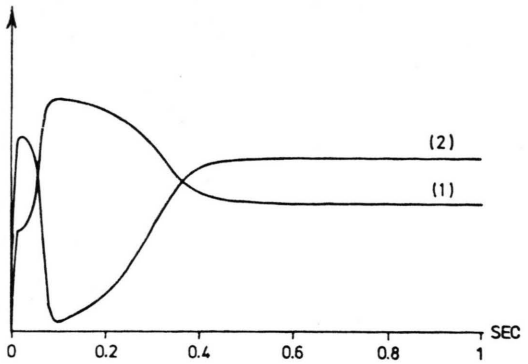

Fig. 4 c. Fluorescence (1) and oxygen evolution (2) induction curve calculated for a dark adapted photosynthetic system with $k_6=0$ (Fig. 1) and with a bypass from PQ to P 700 according to DBMIB block and *p*-PhD bypass *in vivo*.

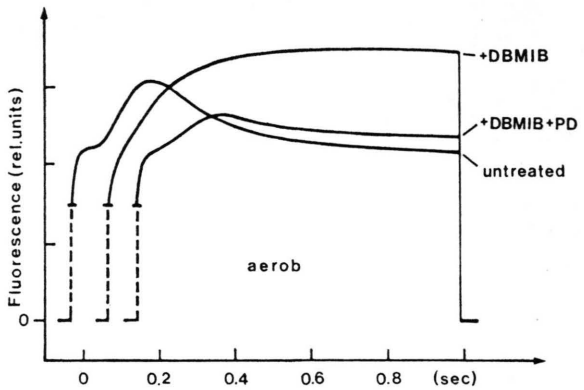

Fig. 4 e. The restoration of the Kautsky effect after the addition of *p*-PhD (5×10^{-4} M) to DBMIB inhibited (5×10^{-5} M) *Scenedesmus* cells [18]. Temperature 25 °C.

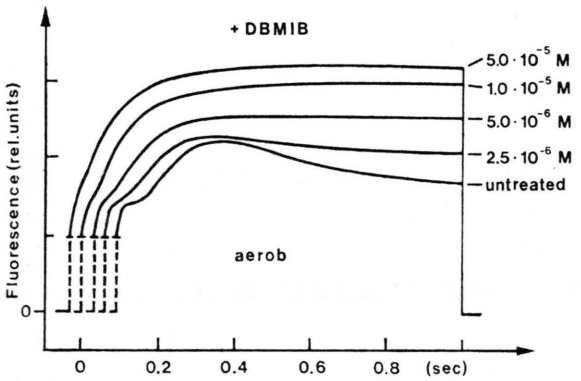

Fig. 4 d. Effect of different concentrations of DBMIB on the fluorescence transients of *Scenedesmus obliquus* [18]. Temperature 25 °C.

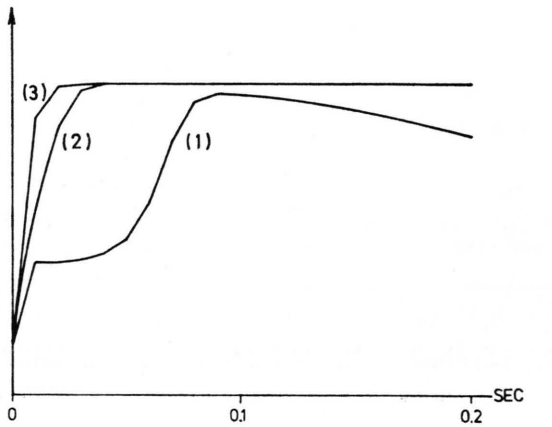

Fig. 5 a. Fluorescence induction curve calculated for a dark adapted photosynthetic system without any block (1), with $k_6=0$ according to DBMIB block *in vivo* (2), and with $k_4=0$ according to DCMU block *in vivo* (3).

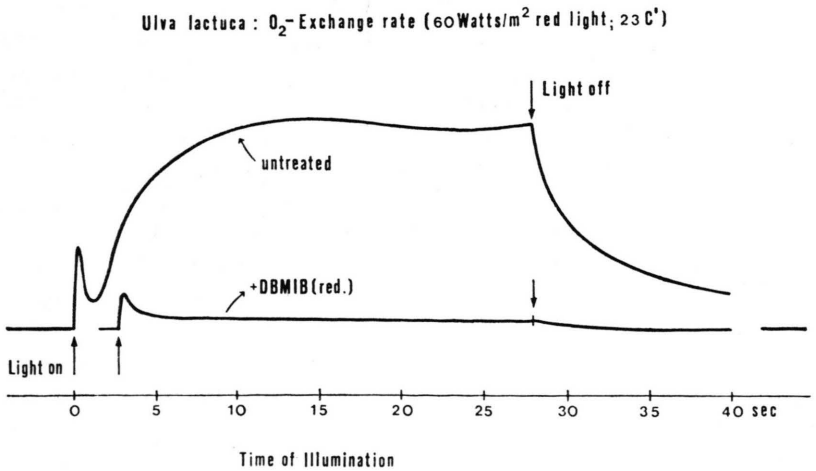

Fig. 4 f. Oxygen evolution induction curve measured with *Ulva lactuca*. A piece of *Ulva lactuca* was placed directly on a Clark type oxygen electrode (Yellow Springs Instruments) with an O-ring. The electrolyte was seawater. The upper curve shows the oxygen evolution without DBMIB, the lower curve shows the influence of DBMIB.

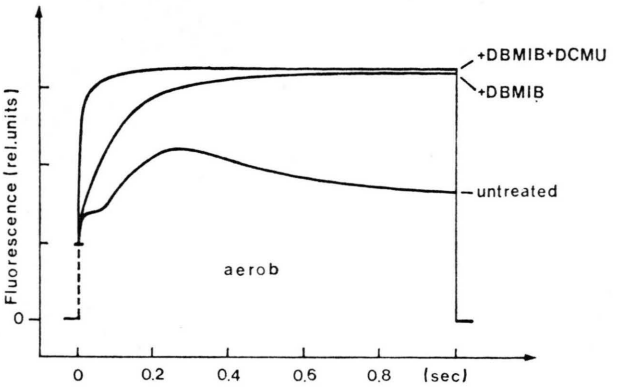

Fig. 5 b. Measured effect of DBMIB (5×10^{-5} M) and DBMIB plus DCMU (5×10^{-6} M) on the fluorescence transient of *Scenedesmus obliquus* [18]. Temperature 25 °C.

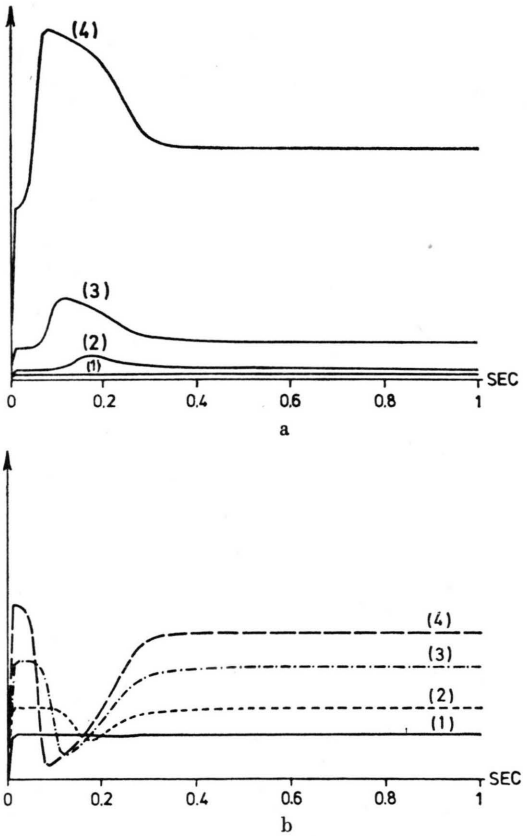

Fig. 6. Fluorescence (Fig. 6 a) and oxygen evolution (Fig. 6 b) induction curves calculated for a dark adapted photosynthetic system without any block at different light intensities: 1 mW/cm² (1), 2 mW/cm² (2), 5 mW/cm² (3), and 20 mW/cm² (4). Alle the curves in Figs 2—5 and 8 are calculated with a light intensity of 10 mW/cm².

oxygen evolution measured with *Ulva lactuca*.

The rise of $[Q^-]$ is still quicker with $k_4 = 0$ (DCMU) than it is with $k_6 = 0$ (DBMIB or mut.

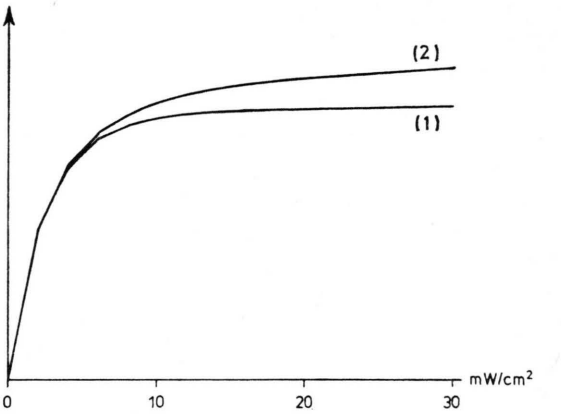

Fig. 7. Oxygen evolution (arbitrary units) in dependence on light intensity calculated for a photosynthetic system in steady state for two different values of k_{12} (Fig. 1), k_{12} low (1) and k_{12} high (2).

No. 8). Fig. 5 a shows the calculated curves of these two cases compared with the case of unblocked electron flow. Fig. 5 b shows the experimental curves measured with *Scenedesmus obliquus* [18].

The peak P in $[Q^-]$ does not occur at lower light intensities. Fig. 6 shows $[Q^-]$ and $[Z^+]$ at different light intensities. At lower light intensity the efflux of electrons from Q is big enough, as compared to the influx into Q, to prevent pile-up. This conforms with experimental findings [5, 9]. The dependence of the steady state value of $[Z^+]$ *i. e.* oxygen evolution on the light intensity shows the features of the light curve (Fig. 7). It also shows that the value of the coefficient k_{12} influences the saturation value of the photosynthetic process, which corresponds to the influence of a high light factor as for example the concentration of CO_2. In fact, the model supports the conclusion of Mitscherlich rather than that of Blackman [24]. The steady state electron flux is given by

$$f = k_0[Z^+]_s = k_1[\text{PS II}^*]_s[Z]_s[Q]_s = k_4[Q^-]_s[X]_s = \ldots \qquad (13)$$

and the maximal possible flux between the pools in *e. g.*

$$f_{max}(Z \rightarrow Q) = k_1[\text{PS II}_0][Z_0][Q_0] \qquad (14)$$

or

$$f_{max}(Q \rightarrow X) = k_4[Q_0][X_0] .$$

The influence of a coefficient k on the steady state flux f depends on the difference between the maximal possible flux f_{max} and the real flux f. The smaller f is compared to f_{max} the greater is the influence of that k-value belonging to f_{max}.

The initial values of the pools are set according to their redox level in the dark adapted state. In the aerobic case the plastoquinone pool PQ is reduced to about 50%[15], which implies that the pools Cyt f and P 700 must be reduced to a high extent; in the calculations an initial reduction of 100% was used for Cyt f and P 700. All the other pools are "empty", *i. e.* Q, X, FD, and $NADP^+$ are totally oxidized, Z is totally reduced and the initial ATP level is zero. In the anaerobic case the pools are partially reduced to a higher extent than they are in the aerobic case (explanation for this see ref. 17 resp. 25 and 26).

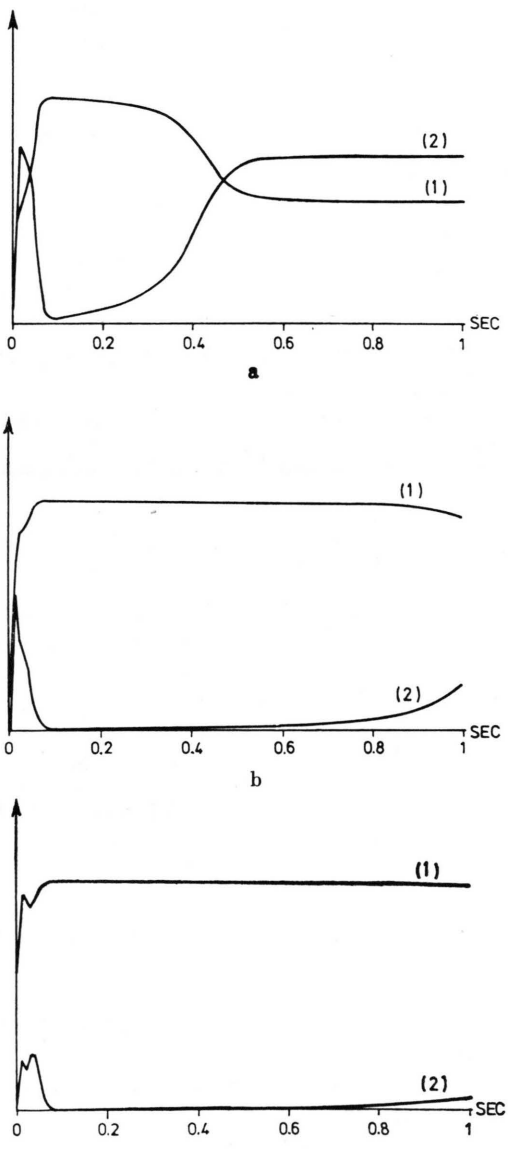

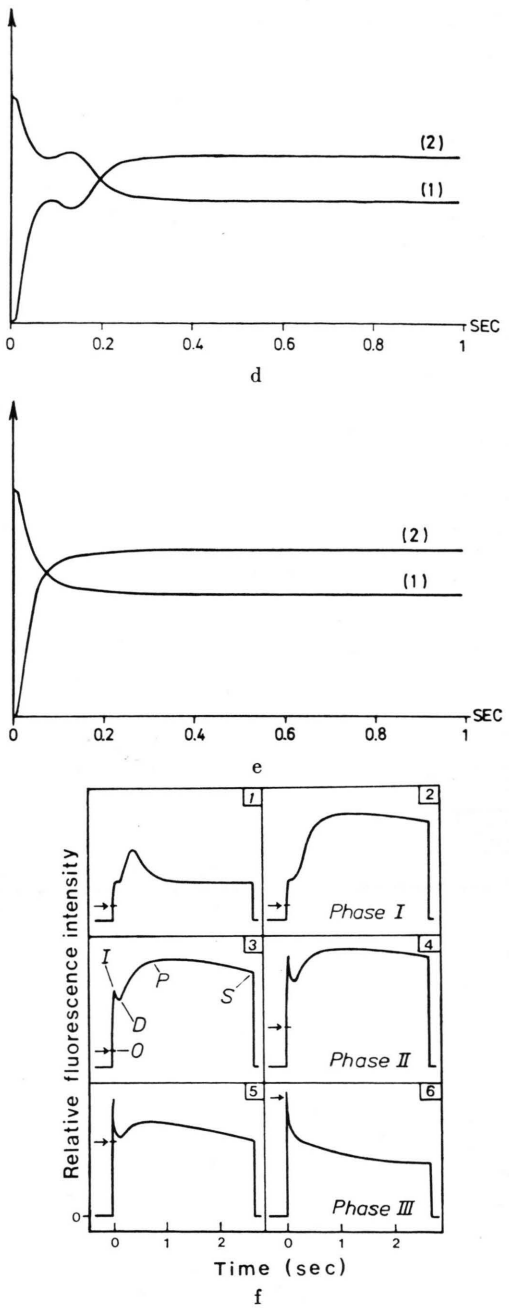

Fig. 8. Fluorescence (1) and oxygen evolution (2) induction curve calculated for a dark adapted photosynthetic system under anaerobic conditions: 8 a: PQ 83% reduced and FD 50% reduced; 8 b: PQ and FD 100% reduced and X 50% reduced; 8 c: PQ, FD, and X 100% reduced and Q 50% reduced; 8 d: PQ, FD, X, and Q 100% reduced and ATP level at 50% of pool size; 8 e: PQ, FD, X, and Q 100% reduced and ATP level at 100%; 8 f: Measured fluorescence transients of *Scenedesmus obliquus* during increasing oxygen removal (flushing the sample with N_2/CO_2). The isolated fluorescence decrease in phase III reflects exclusively the oxidation of Q by PS I [25, 26].

The measured fluorescence induction curve with increasing anaerobism [25, 26] shows that the first step is a very much slower decrease from the P-peak to the steady state S-level. This means in our model that the electron flux is blocked after P Q for the same time as it takes to establish the S-level. If we assume that FD is reduced in the dark under anaerobic conditions, then this would block the flux for a longer time because the initial level of ATP at the onset of illumination is not high enough to induce the oxidation of $NADPH_2$ which is reduced immediately by FD.

Figs 8 a and 8 b show the slower decrease from P to S at higher initial reduction levels of P Q and FD. The next step shows an increase of the D depression and of the first maximum I, which is caused by a higher initial reduction value of X (Figs 8 b and 8 c). Furthermore, with progressive anaerobism the initial fluorescence value O increases, which is caused by a higher initial reduction of the quencher Q (Fig. 8 c and Fig. 8 d).

With further increasing anaerobism the delay in the P – S transient disappears again. This must be caused by an increasing energy source providing ATP for dark reactions which lead to the oxidation of $NADPH_2$. Figs 8 d and 8 e show the influence of a higher ATP level at the onset of illumination. The isolated fluorescence transient (Fig. 8 e) is caused by the oxidation of the totally reduced quencher Q due to the oxidation of $NADPH_2$ which oxidizes successively the whole electron transport chain back to Q [26]. Note the initial delay in the oxidation of Q of about 20 msec which is the time the electron holes need to migrate back from $NADPH_2$ to Q.

Fig. 8 f shows the experimental data of the influence of increasing oxygen removal on the fluorescence induction transient [25]. Phase I corresponds to the case in Fig. 8 b of the model, phase II to Fig. 8 c, and phase III corresponds to Fig. 8 e.

Discussion

Already the modelling of the simplest form of the Z-scheme as presented here shows in many respects very good agreement with experimental results. The modelling presented in this paper describes the induction curve of fluorescence and oxygen evolution. From this point it is not too difficult to expand the modelling to describe the more complicated concepts of primary processes as for example the four step mechanism of oxygen evolution [12–14], the two phase reoxidation of plastoquinone [1, 15], the possible switch in electron acceptance between $NADP^+$, oxygen, and the component for the cyclic photophosphorylation [27].

The four step mechanism of the water splitting system was replaced by the simple assumption that the oxygen evolution *i. e.* the rate of water splitting is proportional to the amount of oxidized Z. According to Forbush, Kok, and McGloin [13] oxygen evolution corresponds to the concentration of S_3-states. In the steady state of this four step mechanism the concentrations of all four S-states are equal [14]. This steady state is established after a longer series of flashes or after continuous illumination in a time less than 1 msec. This can be estimated from the fact that the steady state is reached after about 20 flashes with a duration of 10 μsec each, giving 0.2 msec [14]. Thus the time scale of establishing the steady state of the four step mechanism of the water splitting system does not interfere with the time scale considered in this paper, in which fluorescence induction and induction of oxygen evolution occur. The oxygen evolution therefore is a function of the amount of oxidized Z

$$O_2\text{-evol.} = f(S_3) = f(\tfrac{1}{4}[Z^+]). \qquad (15)$$

In fact this function is not linear [28] as it is assumed in this paper. However, this only means a quantitative change of oxygen evolution in the figures, not a qualitative change in the behaviour of the induction curves.

The more complicated reduction and two step reoxidation of plastoquinone [1, 15, 29–32] was replaced by the simple second order reduction and reoxidation as described by Eqn (3). This only results in a different behaviour of the reoxidation of plastoquinone in the dark, the P – S transition in the fluorescence induction curves is not affected by this simplifications. The reduction of plastoquinone shows a difference in the behaviour of the model as compared to experimental data [32]. The reduction in the model is too slow in the first 20 msec, later it is too quick. However, the time scale is still the same – the time of 100% reduction of P Q is some 0.1 sec in our model. The transition time to the P-peak in the fluorescence induction curve anyway varies much more amongst different species [5].

The mechanism of phosphorylation is summarized in the formation of ΔpH which leads to

the formation of ATP. We did not consider the field formation in the model, neither the question whether the electric field across the membrane or/and the pH difference leads to ATP formation [1]. The main point of the mechanism is the delay between onset of light and the fead back *via* ATP formation which leads to the P – S transition in the fluorescence induction curve.

Also, only the noncyclic photophosphorylation is considered since this is the main process in normal aerobic conditions [27, 33]. The cyclic phosphorylation occuring under anaerobic conditions may be the source of ATP we have to assume in the last anaerobic stages in Figs 8 d and 8 e. But it is difficult to see how in the dark ATP can be provided.

Neither clear is the fact that the fluorescence is quenched if the electron flux is blocked as in DCMU treated anaerobic wildtype algae or in anaerobic mutant No. 11 of *Scenedesmus obliquus* which is blocked in PS II activity [22, 25].

We are aware of the fact that the terminus "primary" is related to the redox processes and not to the much quicker processes described by Mauzerall [34]. The primary redox processes considered in this paper are related to the states F_2 or F_3 and later states [34].

The process $F_3 \rightarrow F_4$ is thought of to correspond to the reduction of the quencher Q. This should occur in a few μsec. The process $F_4 \rightarrow F_5$ is correlated to the reoxidation of Q by the reduction of P Q in the time 0.5 msec, *i. e.* the process $F_3 \rightarrow F_4$ is related to the first increase $O \rightarrow I$ and the process $F_4 \rightarrow F_5$ is related to the first decrease $I \rightarrow D$ in the fluorescence induction curve. The difference in the time scale is caused by the fact that in the flash experiments the redox states of the pools are only changed partially, whereas in continuous light it takes a much longer time to establish the quasi-steady states I, D, and later P. The time of 90% reduction of P Q or reoxidation of Q is about 0.1 sec or more [32] which we also are able to calculate from the model. The half time of P Q reduction is 0.6 msec according to Witt [1], which is in good agreement with the time of the process $F_4 \rightarrow F_5$ [34].

[1] H. T. Witt, Quart. Rev. Biophys. **4**, 365 [1971].
[2] H. T. Witt, B. Rumberg, and W. Junge, Biochemie des Sauerstoffs (H. Staudinger and B. Hess, ed.), p. 262, Springer-Verlag, Berlin, Heidelberg, and New York 1968.
[3] W. Vidaver and Tr. Chandler, Progress in Photosynthesis Research (H. Metzner, ed.), **Vol. I**, p. 514, Tübingen 1969.
[4] A. Ried, Progress in Photosynthesis Research (H. Metzner, ed.), **Vol. I**, p. 521, Tübingen 1969.
[5] U. F. Franck, N. Hoffmann, H. Arenz, and U. Schreiber, Ber. Bunsenges. Phys. Chem. **73**, 871 [1969].
[6] S. Malkin and B. Kok, Biochim. Biophys. Acta **126**, 413 [1966].
[7] S. Malkin, Biochim. Biophys. Acta **126**, 433 [1966].
[8] J. C. Munday and Govindjee, Biophys. J. **9**, 1 [1969].
[9] N. Hoffmann, Thesis, T.H. Aachen 1967.
[10] D. S. Bendall, H. E. Davenport, and R. Hill, Methods of Enzymology (A. San Sietro, ed.), **Vol. XXIII**, p. 327, Academic Press, New York, London 1971.
[11] W. Cramer and P. Horton, Proc. IIIrd Int. Congress on Photosynthesis, Rehovot, Israel 1974.
[12] B. Kok, B. Forbush, and M. McGloin, Photochem. Photobiol. **11**, 457 [1970].
[13] B. Forbush, B. Kok, and M. McGloin, Photochem. Photobiol. **14**, 307 [1971].
[14] P. Joliot,, A. Joliot, B. Bouges, and G. Barbieri, Photochem. Photobiol. **14**, 287 [1971].
[15] P. Schmidt-Mende and H. T. Witt, Z. Naturforsch. **23 b**, 228 [1968].
[16] U. F. Franck and N. Hoffmann, Progress in Photosynthesis Research (H. Metzner, ed.), **Vol. II**, p. 899, Tübingen 1969.
[17] R. Bauer, Thesis, T.H. Aachen 1972.
[18] R. Bauer and M. J. G. Wijnands, Z. Naturforsch. **29 c**, 725 [1974].
[19] Govindjee and G. Papageorgiou, Photophysiology (A. C. Giese, ed.), **Vol. VI**, p. 1, Academic Press, New York, London 1971.
[20] T. T. Bannister and G. Rice, Biophys. Biochim. Acta **162**, 555 [1968].
[21] L. N. M. Duysens, IInd Int. Congress on Photosynthesis Research (G. Forti *et al.*, eds.), **Vol. I**, p. 19, Dr. W. Junk N. V. Publishers, The Hague 1972.
[22] N. I. Bishop, Methods of Enzymology (A. San Pietro, ed.), **Vol. XXIII**, p. 130, Academic Press, New York, London 1971.
[23] A. Trebst and S. Reimer, Z. Naturforsch. **28 c**, 710 [1973].
[24] M. G. Stålfeld, Handbuch der Pflanzenphysiologie (W. Ruhland, ed.), **Vol. V/2**, p. 213, Springer-Verlag 1960.
[25] U. Schreiber, R. Bauer, and U. F. Franck, IInd Int. Congress on Photosynthesis Research (G. Forti *et al.*, eds.), **Vol. I**, p. 169, Dr. W. Junk N. V. Publishers, The Hague 1972.
[26] R. Bauer and U. F. Franck, Proc. IIIrd Int. Congress on Photosynthesis, Rehovot, Israel 1974.
[27] U. Heber,, Ber. Deutsch. Bot. Ges. **86**, 187 [1973].
[28] M. Delrieu, Photochem. Photobiol. **20**, 441 [1974].
[29] J. Vater, Thesis, T.H. Berlin 1971.
[30] H. H. Stiehl, Thesis, T.H. Berlin 1969.
[31] H. H. Stiehl and H. T. Witt, Z. Naturforsch. **23 b**, 220 [1968].
[32] P. Schmidt-Mende and B. Rumberg, Z. Naturforsch. **23 b**, 225 [1968].
[33] E. Rabinowitch and Govindjee, Photosynthesis, J. Wiley and Sons Inc., New York 1969.
[34] D. Mauzerall, Proc. Nat. Acad. Sci. U.S. **69**, 1358 [1972].